

# Crystal Habit Modification of Vitamin C (L-Ascorbic Acid) due to Solvent Effects

Ali ARSLANTAŞ<sup>1\*</sup>, Walter C. ERMLER<sup>1</sup>, Rahmi YAZICI<sup>2</sup>, Dilhan M. KALYON<sup>2</sup>

<sup>1</sup>*Department of Chemistry and Chemical Biology of Stevens Institute of Technology,  
Hoboken, New Jersey 07030, USA*

<sup>2</sup>*Highly Filled Materials Institute (HFMI), Stevens Institute of Technology,  
Hoboken, New Jersey 07030, USA*

Received 25.09.2001

Crystal morphologies are predicted for vitamin C (L-ascorbic acid) using attachment energy methods. The significant differences between predicted and observed morphologies when vitamin C is grown from water, isopropyl alcohol, acetone-water solution, and isopropyl alcohol-methanol solution are attributed to the effect of solvent on the growth rate of the various crystal habit faces. This effect, particularly the role of hydrogen bonding between solvent and crystal surface, is examined. Molecular modeling is combined with the results of simple experiments charting the habit shift of vitamin C as a function of the hydrogen bonding tendency of the solvent or solvent mixture. Attachment and slice energies can be determined from periodic bond chain (PBC) analysis or calculated directly from the crystal structure by partitioning the lattice energy calculated from each symmetrically independent molecule in the unit cell into slice and attachment energies. First in the PBC analysis of vitamin C the Cerius<sup>2</sup> molecular modeling package was used to search for connected nets in a given range of orientations (hkl).

## Introduction

All of the electronic properties of a drug are determined by the atomic composition, shape and size of the drug molecule and its structure<sup>1</sup>. The crystallography of small organic and inorganic molecules is of technological importance in characterization, in the expression of physical properties and in the processing and formulation of organic and inorganic crystalline compounds such as drugs, pigments and chemicals<sup>2</sup>. Organic morphology control is important for many applications in the chemical industry, such as the control of particle size<sup>3</sup>.

The unique features of L-ascorbic acid include acidity without a carboxyl group, an unusually stable  $\gamma$ -lactone ring, its reducing power, and 2 chiral carbon atoms. With the advent of modern methods in crystallography the detailed geometries of ascorbates became accessible and a number of structures are known. These investigations generally confirmed the predicted chemical formula and bonding properties of the ascorbates<sup>4</sup>. Vitamin C (C<sub>6</sub>H<sub>8</sub>O<sub>6</sub>, see Figure 1) was the first ascorbate to be studied in detail by diffraction methods<sup>5,6</sup>. It crystallizes in the monoclinic space group P2<sub>1</sub> with 2 molecules in the unit cell<sup>5,7</sup>.

\*Present Address: Department of Chemistry, Kafkas University, 36100, Kars-Turkey

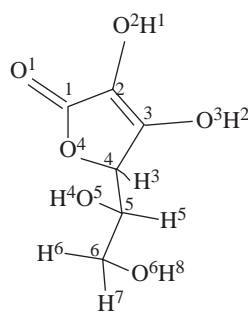


**Figure 1.** L-Ascorbic acid molecule ( $C_6H_8O_6$ ).

There has been increasing interest in the prediction of crystal structures on the basis of molecular information only. A variety of theoretical methods have been developed to generate possible crystal structures<sup>8</sup>. There will often be a large number of possible crystal structures, as judged from their lattice energy. Crystal habit has a great impact on solid/liquid separation, processability, and the crystal surface environment chemistry of a material. As purity, cost of manufacture, and end-use properties are affected, it is very important to be able to predict and control the crystal habit. Crystal habit modeling has advanced to the state where habit prediction for organic materials is relatively straightforward. However, significant differences between predicted and actual habit are frequently encountered for solution grown materials. This is because standard crystal habit modeling does not take into account interactions between the growing crystal and the surrounding solution<sup>9</sup>. For vitamin C crystallized from common solvents, solvent/crystal interactions significantly affect the crystal habit. In particular, hydrogen bonding between vitamin C and the solvent plays a large role in determining the crystal growth habit. In addition, Hartman and Bennema<sup>10</sup> looked at attachment energy as a habit-controlling factor. They found that the relative growth velocity always increases with increasing  $E(Att)$ ; however, the relationships between them depend on the mechanism of crystal growth and variables such as supersaturation, temperature, and solid-fluid interaction. Hartman and Bennema<sup>10</sup> demonstrated at low supersaturation, however, that the relative growth velocity of a face is directly proportional to the attachment energy of that face. In crystals grown from solution, the solvent can greatly influence the crystal habit due to small amounts of impurities. Discrepancies between the observed crystal habit and those obtained using attachment energies have been accounted for by assuming preferential solvent (or impurity) adsorption on crystal faces<sup>11</sup>.

In this study we investigated the solvent effects on the crystal habit modification of vitamin C (L-ascorbic acid) using a series of solvents, including water, isopropyl alcohol, acetone-water, and isopropyl alcohol-methanol, enhanced through the use of computational chemistry methods.

## Experimental Procedure

Crystals were grown at ambient temperature by slow solvent evaporation for the 4 solvents and 4 solvent mixtures. The evaporation rate of the solvent was controlled by partially covering the top of a small beaker containing L-ascorbic acid solution and controlling the amount of open area. The open area was adjusted to give approximately the same growth rate for each of the solvents studied, adjusting for the relative volatility of the solvent used. Recrystallization and crystal growth with controlled temperature using solutions concentrated less than saturated of L-ascorbic acid were studied. Single crystal X-ray diffraction and wide angle X-ray diffraction experiments and optical microscopy methods were performed. Crystal

structure predictions of vitamin C and the study of solvent effects on crystal morphology and hydrogen bonds were carried out using computational chemistry. The Cerius<sup>2</sup> molecular modeling package was used to obtain predictions.

In this study 4 solvents were chosen (water, methanol, acetone and isopropyl alcohol). These solvents exhibit a range of polarity and therefore hydrogen bonding potential.

**List of Chemicals:** methanol (Merck), acetone (Merck) isopropyl alcohol (Merck) and L-ascorbic acid (Merck).

**List of Instruments:** Wide-angle X-ray diffractometer (Nonius), single-crystal X-ray diffractometer (Kappa Diffractometer) and the Cerius<sup>2</sup> Molecular Modeling Package (Molecular Simulation Inc.).

### 1. Recrystallization from isopropyl alcohol

First 0.5 g of L-ascorbic acid was weighed and transferred into a 150 mL beaker and 5 mL of isopropyl alcohol was added to the sample until it dissolved. The resulting solution of L-ascorbic acid and isopropyl alcohol was then heated slowly on a water bath to ensure that all the sample was completely dissolved. The crystals of vitamin C were grown at room temperature by slow solvent evaporation from the solvent, with the system isolated from mechanical vibrations. Over a 2-week period, needle-shaped crystals of vitamin C were produced. The experiment was repeated 3 times. Wide-angle X-ray diffraction measurements were performed on the crystals and compared with the diffraction data in the literature<sup>6</sup>. Finally, the best-shaped crystal was chosen to determine the cell parameters of the material using single-crystal X-ray diffractometer.

### 2. Recrystallization from acetone-water

A sample of 0.5 g of L-ascorbic acid was weighed and transferred into a 50 mL beaker, 5 mL of acetone was added to the sample until it dissolved, and a few milliliters of distilled water was added to the solution. Then the solution was checked to ensure that all the L-ascorbic acid sample was completely dissolved. The other parts of the experiment were the same as those in experiment 1.

### 3. Recrystallization from isopropyl alcohol-methanol

A 0.5 g sample of L-ascorbic acid was weighed and transferred into a 50 mL beaker. Initially 5 mL of isopropyl alcohol was added to the sample until it dissolved, and then methanol was added to the system. The solution was then heated slowly to ensure that the sample was completely dissolved. The other parts of the experiment were the same as those in experiment 1.

### 4. Recrystallization from distilled water

A 0.5 g sample of L-ascorbic acid was weighed and transferred into a 50 mL beaker and 5 mL of distilled water was added to the sample until dissolution, and additional vitamin C was added to the system until supersaturation. The other parts of experiment were the same as those in experiment 1.

## Results And Discussion

Figures 2-5 shows vitamin C crystals grown from isopropyl alcohol, acetone-water and isopropyl alcohol-methanol and water. In Figure 6 (a, b, c, d) the observed morphologies of the crystals are given for comparison purposes. For the water grown crystals,  $\{0\ 0\ 1\}$  is the dominant face. For the isopropyl alcohol growth crystals,  $\{0\ 0\ 1\}$  is also the dominant face, but the area of this face is smaller than that of vitamin C grown in water. For the acetone-water grown crystals the dominant faces are  $\{0\ 0\ 1\}$  and  $\{1\ 0\ 0\}$ . The dominant face of vitamin C grown in isopropyl alcohol-methanol is again the  $\{0\ 0\ 1\}$  face. To further probe

the effect of solvent polarity, vitamin C crystals were grown from mixtures of acetone and water. There is a slight change in the relative areas of the faces as the solvent polarity increases from acetone to water, methanol, and isopropyl alcohol.

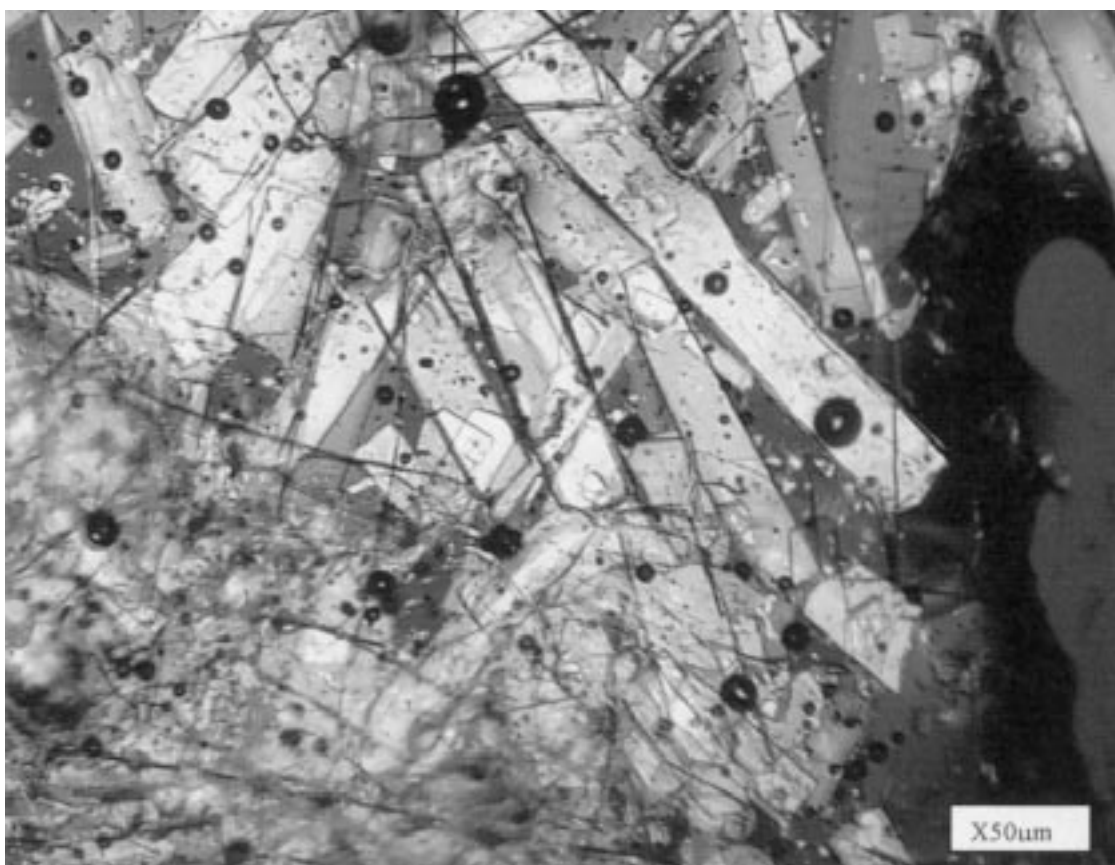


**Figure 2.** Vitamin C crystals grown by slow evaporation from isopropyl alcohol.

In some studies habit predictions are based on lattice geometry<sup>12–14</sup> and attachment energy using the force fields of Lifson<sup>15</sup>, Momany et al.<sup>16,17</sup> and Scheraga<sup>18</sup>. The Cerius<sup>2</sup> molecular modeling package was used to obtain predictions<sup>15</sup>. There are slight differences among the habit predictions using lattice geometry and those from the 4 force fields studied (see Figures 6-15), with the most obvious perhaps being the presence or absence of the  $\{0\ 2\ 0\}$  face. The lattice geometry and Lifson predictions have the  $\{0\ 2\ 0\}$  face, while the Momany and Scheraga, and Dreiding predictions do not. Previously, we found the attachment energy prediction using the force field of Dreiding to be the best fit to the water-grown crystal habit. The attachment energy prediction using the Lifson force field is a better fit to the acetone-water grown crystal habit, although the  $\{0\ 2\ 0\}$  face not present in the growth morphology is present in the prediction.



**Figure 3.** Vitamin C crystals grown by slow evaporation from acetone-water.

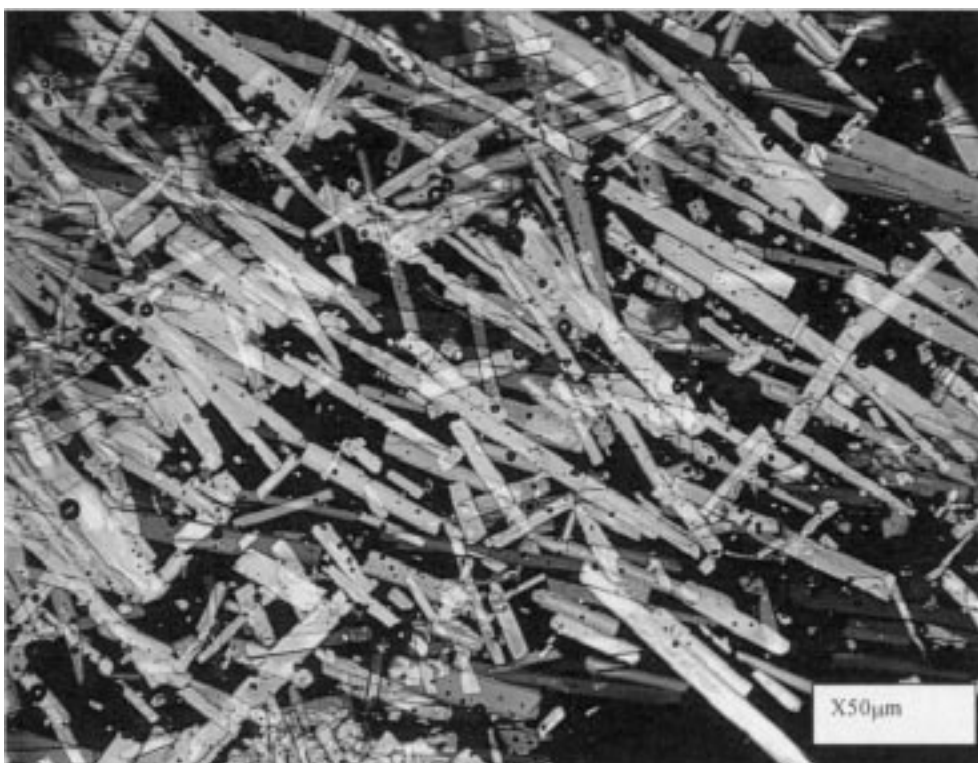


**Figure 4.** Vitamin C crystals grown by slow evaporation from isopropyl alcohol-methanol.

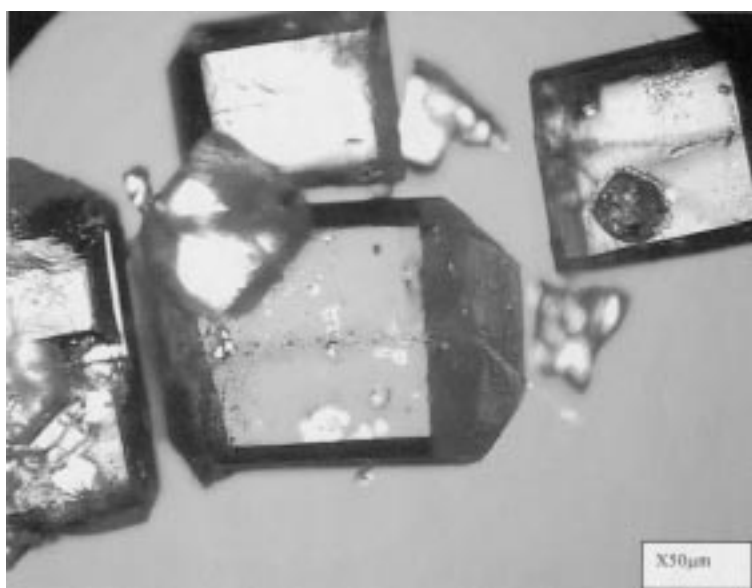


**Figure 5.** Vitamin C crystals grown by slow evaporation from water.

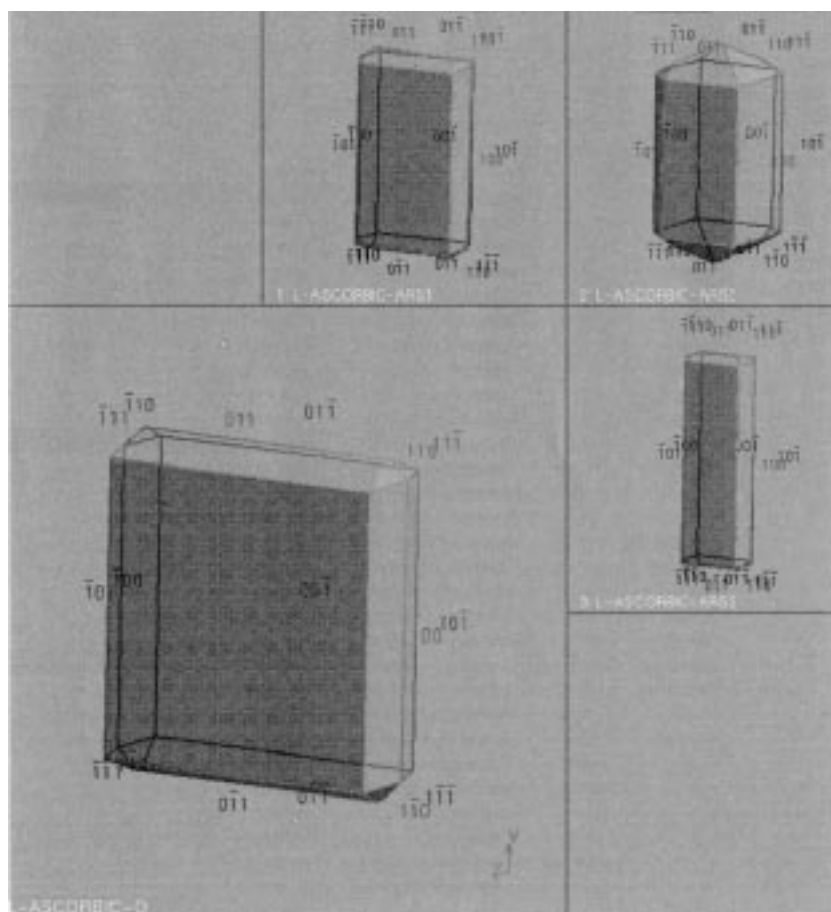


**Figure 6.** Observed morphologies for vitamin C crystals grown by slow evaporation from a) water, b) isopropyl alcohol, c) acetone-water, and d) isopropyl alcohol-methanol.

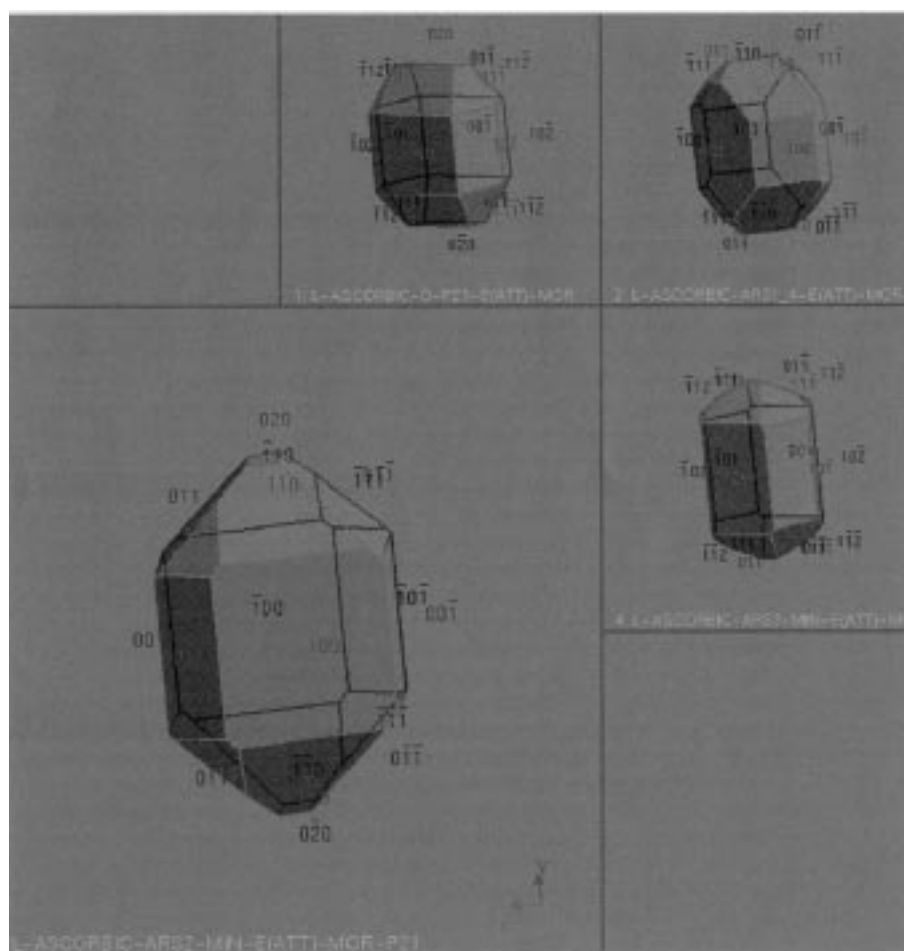


**Figure 7.** Predicted vitamin C crystal morphologies based on attachment energy force field of Dreiding a) water, b) isopropyl alcohol, c) acetone-water, and d) isopropyl alcohol-methanol.

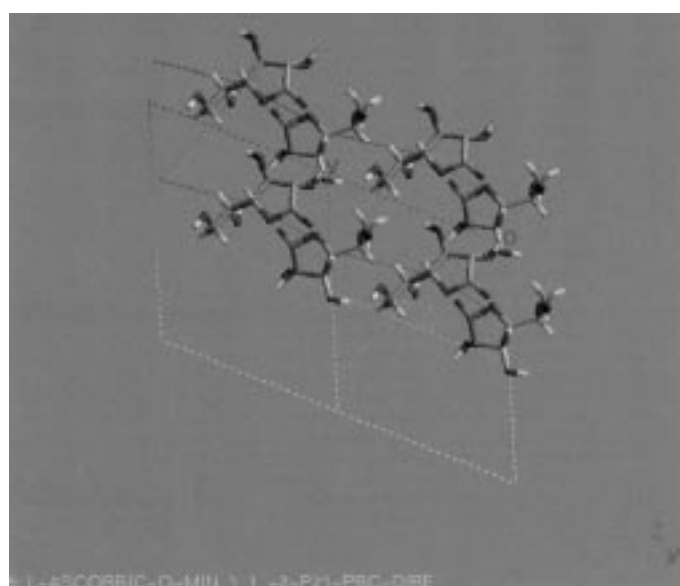


**Figure 8.** Visualization of a connected net for {1 1 -2} of Vitamin C crystals grown by slow evaporation from water.

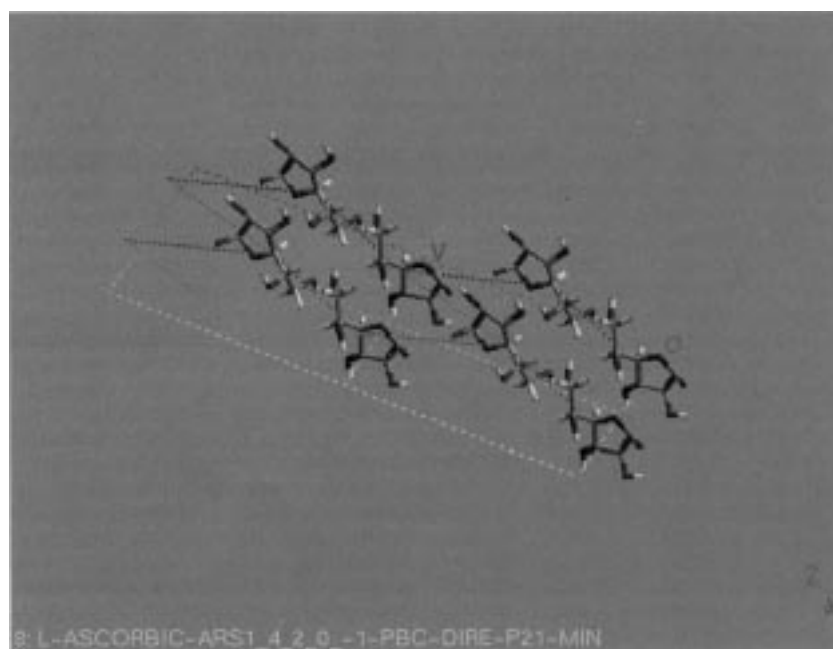


**Figure 9.** Visualization of a connected net for  $\{2\ 0\ -1\}$  of vitamin C crystals grown by slow evaporation from isopropyl alcohol.

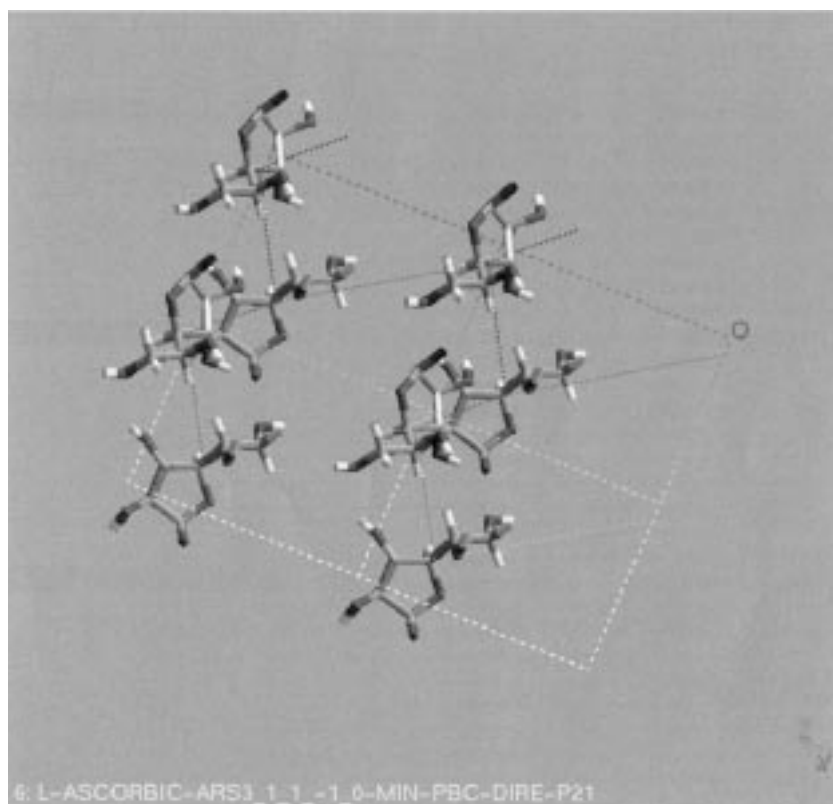


**Figure 10.** Visualization of a connected net for  $\{1\ 1\ -1\}$  of vitamin C crystals grown by slow evaporation from acetone-water.

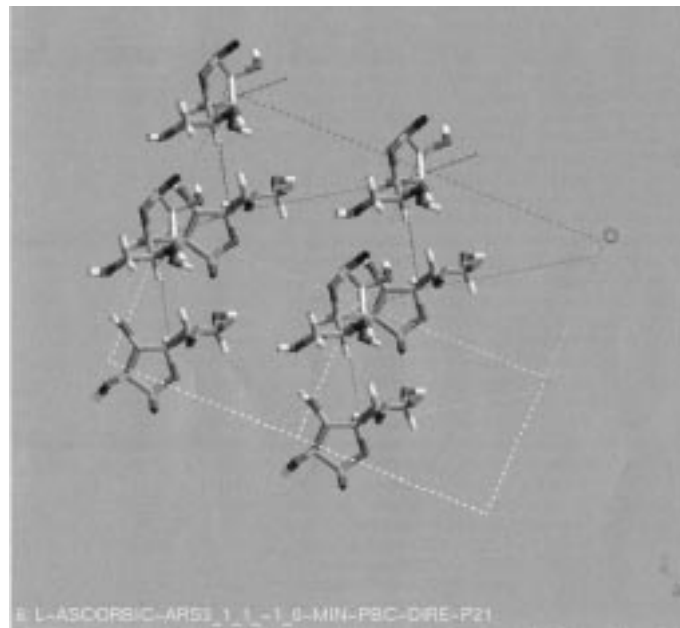


**Figure 11.** Visualization of a connected net for  $\{1 -1 0\}$  of vitamin C crystals grown by slow evaporation from isopropyl alcohol-methanol.

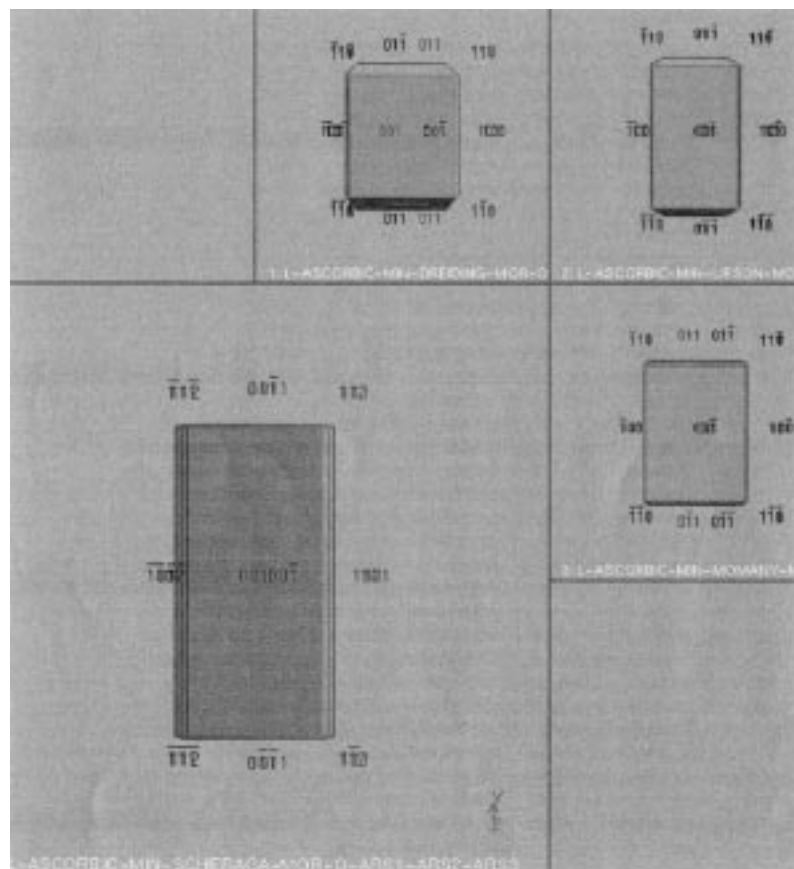


**Figure 12.** Predicted vitamin C crystal morphologies from water based on force field of a) Dreiding, b) Lifson, c) Scheraga, and d) Momany.

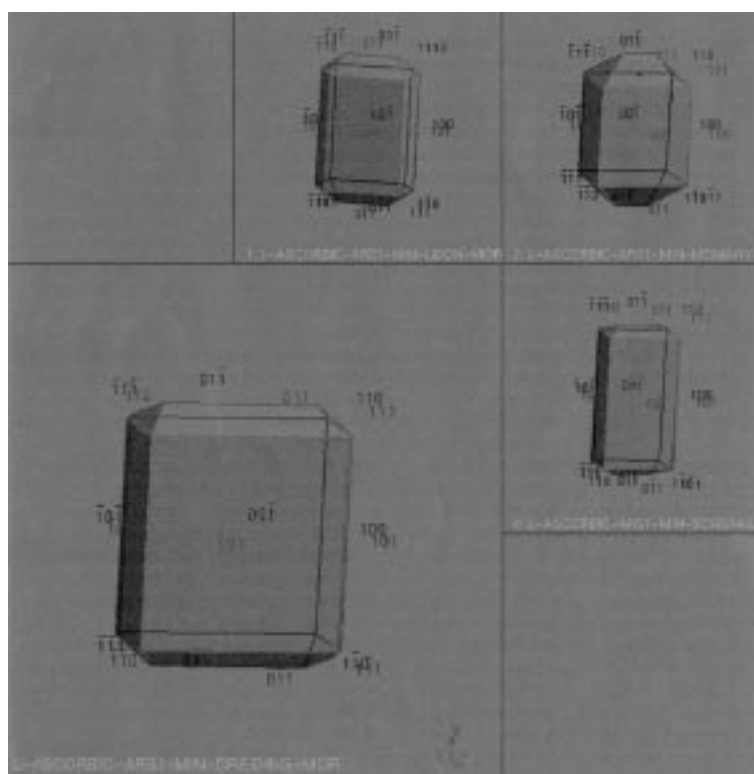


**Figure 13.** Predicted vitamin C crystal morphologies from isopropyl alcohol based on force field of a) Dreiding, b) Lifson, c) Scheraga, and d) Momany.

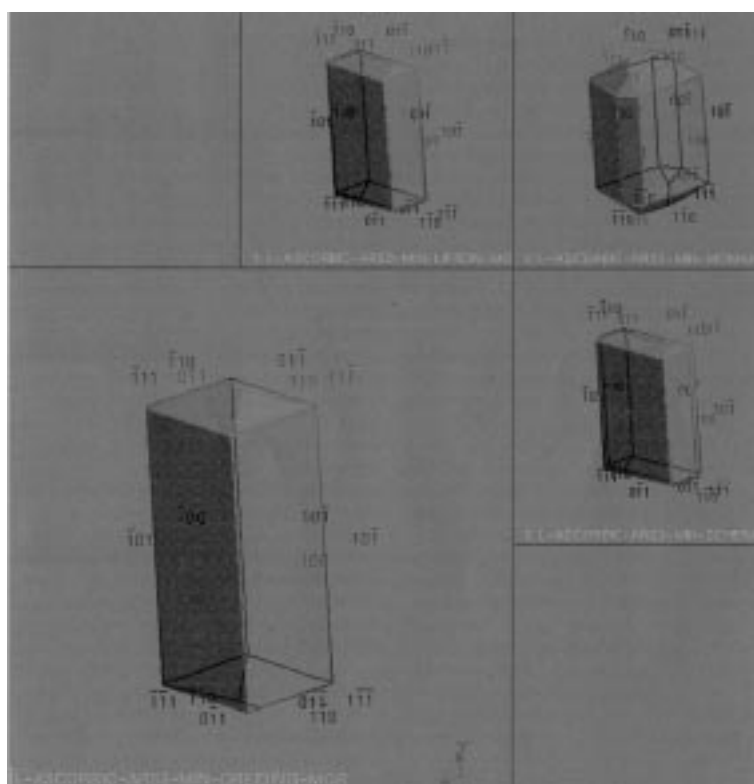


**Figure 14.** Predicted vitamin C crystal morphologies from isopropyl alcohol-methanol based on force field of a) Dreiding, b) Lifson, c) Scheraga, and d) Momany.

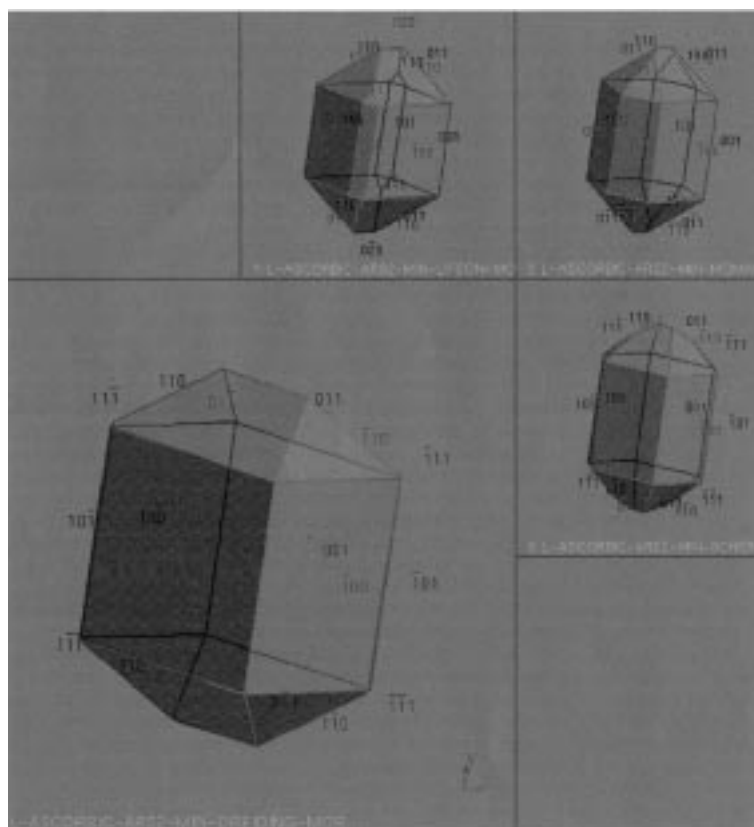


**Figure 15.** Predicted vitamin C crystal morphologies from acetone-water based on force field of a) Dreiding, b) Lifson, c) Scheraga, and d) Momany.

The attachment energy is defined as the energy released on attachment of a particular growth slice onto the surface in a specified orientation. Faces with the lowest attachment energies will be the slowest growing and therefore will be the morphologically most important. The molecular modeling package Cerius<sup>2</sup> was used<sup>16</sup> for the calculation of attachment energies. This module is based on the method described by Bravais<sup>19</sup>. The attachment energy of an F-face  $E_{att}$  is computed as

$$E_{att} = E_{latt} - E_{slice}, \quad (1)$$

where  $E_{latt}$  is the lattice energy of the crystal and  $E_{slice}$  is the energy released on the formation of a growth slice of thickness  $d_{hkl}$ . The attachment energy is then calculated from the highest  $E_{slice}$  using Eq. 1. This procedure is repeated for all growth units in the unit cell and for all orientations (hkl). The attachment energies were calculated for vitamin C using Dreiding force fields. The Dreiding, Lifson, Momany and Scheraga force field parameters were all available in Cerius<sup>2</sup>. The results of the calculations are listed in Tables 1-4.

A well-established method to predict the morphology of a crystal is periodic bond chain (PBC) analysis, developed by Hartman and Bennema<sup>10</sup>. In this approach an assumption is made that there is a high growth rate along directions of strong uninterrupted chains of bonds between the growth units in the lattice<sup>13</sup>. In PBC analysis of vitamin C, Cerius<sup>2</sup> was used to search for connected nets in a given range of orientations (hkl). Figures 8-11 show examples of the connected nets of vitamin C. Generally, the agreement

between predicted and experimentally grown crystal morphologies is good. The overall prediction of a fairly “blocky” crystal, and the identification of the major faces is rather good, particularly for crystals grown from changing seeds by slow cooling, which do not in general, exhibit thinning, probably due to the presence of the glass surface in the evaporative experiments. However, there are significant deviations, and these deviations are found to depend on the solvent used in the crystallization, particularly on the polarity of the solvent and therefore its hydrogen bonding potential. The molecular packing and cell parameters of vitamin C agree with the diffraction data obtained. Images of grown crystals of experiments 1-4 obtained using optical microscopy, are shown in Figures 2-5, respectively.

**Table 1.** Summary of F-faces and attachment energies calculated for vitamin C crystals grown by slow evaporation from water.

Form	type	E(Att) (kcal/mol)	E(Bond) (kcal/mol)
{0 0 1}	1	-12.39	-10.47
{0 0 1}	2	-20.28	-18.20
{1 0-1}	1	-15.28	-13.49
{1 0-1}	2	-15.33	-13.50
{1-1-1}	1	-17.26	-15.05
{0 1-1}	1	-18.02	-15.89
{1 0 0}	1	-18.94	-16.68
{1 0-2}	1	-19.72	-17.54
{1-1 0}	1	-22.10	-20.27
{1-1 0}	2	-24.06	-22.21
{1 1-2}	1	-22.23	-20.49
{0 2 0}	1	-25.12	-23.00
{0 2 0}	2	-25.12	-23.00

**Table 2.** Summary of F-faces and attachment energies calculated for vitamin C crystals grown by slow evaporation from isopropyl alcohol.

Form	type	E(Att) (kcal/mol)	E(Bond) (kcal/mol)
{0 0 1}	1	-12.34	-9.84
{0 0 1}	2	-32.60	-30.16
{0 0 1}	3	-33.10	-30.64
{1 0 0}	1	-16.30	-13.93
{1 0 0}	2	-17.78	-15.33
{1 -1 0}	1	-18.70	-16.11
{1 0 -1}	1	-21.15	-19.70
{1 0 -1}	2	-23.55	-22.05
{1 1 -1}	1	-23.86	-22.36
{0 1 -1}	1	-24.04	-21.48
{0 1 -1}	2	-24.29	-21.72
{0 2 0}	1	-29.32	-27.43
{0 2 0}	1	-29.32	-27.43
{2 -1 -1}	1	-30.21	-27.48
{2 -1 -1}	2	-31.14	-28.41
{2 0 -1}	1	-33.27	-30.26
{0 2 1}	1	-34.68	-31.88

**Table 3.** Summary of F-faces and attachment energies calculated for vitamin C crystals grown by slow evaporation from acetone-water.

Form	type	E(Att) (kcal/mol)	E(Bond) (kcal/mol)
{1 0 0}	-1	-13.98	-12.21
{1 0 0}	-2	-21.77	-20.01
{0 0 1}	-1	-15.89	-14.29
{0 0 1}	-2	-19.75	-81.41
{1 0 1}	-1	-17.43	-15.43
{1 0 1}	-2	-22.51	-21.11
{1 0 1}	-3	-29.02	-27.07
{1 1 0}	-1	-18.89	-16.11
{0 1 -1}	-1	-18.94	-16.35
{1 1 1}	-1	-20.81	-18.27
{1 1 1}	-2	-24.04	-21.25
{1 0 -1}	-1	-24.09	-22.00
{0 2 0}	-1	-24.27	-21.21
{0 2 0}	-2	-24.27	-21.51
{1 1 -1}	-1	-25.20	-21.51
{1 1 -1}	-2	-26.17	-23.43
{1 2 1}	-1	-26.90	-24.09

**Table 4.** Summary of F-faces and attachment energies calculated for vitamin C crystals grown by slow evaporation from isopropyl alcohol-methanol.

Form	type	E(Att) (kcal/mol)	E(Bond) (kcal/mol)
{0 0 1}	-1	-11.54	-9.90
{0 0 1}	-2	-16.24	-14.52
{1 0 -1}	-1	-12.63	-10.83
{1 0 -1}	-2	-15.19	-13.41
{1 0 -2}	-1	-13.53	-11.79
{1 -1 -1}	-1	-18.06	-15.89
{0 1 -1}	-1	-18.14	-15.99
{1 0 0}	-1	-18.67	-16.30
{1 1 -2}	-1	-20.51	-18.93
{1 1 -2}	-2	-22.33	-20.73
{1 -1 0}	-1	-22.69	-20.70
{1 -1 0}	-2	-23.19	-21.21
{0 2 0}	-1	-26.54	-24.33
{0 2 0}	-2	-26.54	-24.33

This effect of solvent polarity can be understood by examining the hydrogen bonding potential of the various crystal faces present in these morphologies. Faces with greater hydrogen bonding potential can be expected to bind more strongly to solvent molecules. For growth of the face to occur, solute molecules must displace hydrogen bonded solvent molecules. Therefore, hydrogen bonding of the solvent to the face must slow the growth rate of that face, and the stronger the hydrogen bonding the greater the retardation of the growth rate of the face.

The faces predicted by both lattice geometry and attachment energy are (Figure 7), approximately, in order of decreasing relative size  $\{0\ 0\ 1\}$ ,  $\{1\ 0\ 0\}$ ,  $\{-1\ 0\ 1\}$ ,  $\{0\ 1\ 1\}$ . Faces observed in the growth morphologies are :  $\{0\ 0\ 1\}$ ,  $\{1\ 0\ 0\}$ ,  $\{0\ 1\ -1\}$  for all crystals, plus  $\{0\ 2\ 0\}$ ,  $\{-1\ 0\ 2\}$ ,  $\{-1\ -1\ 2\}$ ,  $\{-1\ 1\ 2\}$ ,  $\{1\ -1\ 2\}$  and  $\{-1\ -1\ -1\}$  for some of the crystals grown. Differences between all of the growth morphologies and the predictions suggest that the solvent affects the crystal habit for each of the solvents studied, of course to varying degrees.

Examining the position of the molecules in the crystal lattice relative to the crystal faces, particularly the positions of the carbonyl (C=O) and hydroxyl (OH) groups of the vitamin C molecule, which are the preferred sites for hydrogen bonding, we can qualitatively assess the hydrogen bonding potential of the various crystal faces and perhaps rank them from highest to lowest in terms of hydrogen bonding potential. Doing this for the major crystal faces, we get  $\{1\ 1\ -2\}$  (Figure 8) with OH groups projecting above the surface and C=O groups at the surface,  $\{1\ 0\ 0\}$  with OH groups projecting from the surface and carbonyl groups at the surface,  $\{2\ 0\ -1\}$  (Figure 9) with OH groups projecting from and C=O groups near the surface, and  $\{1\ 1\ -1\}$  (Figure 10) and  $\{1\ -1\ 0\}$  (Figure 11) with OH groups projecting from the surface. We expect that the stronger the hydrogen bonding potential of a face the more its growth will be affected by the stronger hydrogen bonding solvents. That is, the growth rate of a strongly hydrogen bonding face will be slowed more by a strongly hydrogen bonded solvent and a more weakly hydrogen bonded solvent. Conversely, the faces showing only weak hydrogen bonding will be slowed less by variations in the hydrogen bonding potential of the solvent. It should be kept in mind that the final growth morphology is the result of the relative growth rates of all the faces.

Considering the habit shift associated with the increasing solvent polarity found for the solvent series water, isopropyl alcohol, acetone-water, and isopropyl alcohol-methanol, the  $\{0\ 0\ 1\}$ ,  $\{1\ 0\ 0\}$  and  $\{1\ 0\ -1\}$  faces increase in relative area with increasing solvent polarity, which is consistent with their strong hydrogen bonding potential.  $\{1\ -1\ -1\}$  and  $\{1\ 1\ -1\}$  faces are observed for water, isopropyl alcohol, acetone-water and isopropyl alcohol-methanol and they have the smallest face size for these solvents. This indicates that these faces grow more relative to the others on the crystal for polar solvents, which is consistent with the comparatively weak hydrogen bonding of the  $\{1\ -1\ -1\}$  and  $\{1\ 1\ -1\}$  faces. The change in the relative area of  $\{0\ 0\ 1\}$  faces results from strong hydrogen bonding. This occurs because of intermediate hydrogen bonding for this face.

If compared to the theoretical crystal habit based PBC analysis (see Figures 8-11), the  $\{1\ 1\ -2\}$ ,  $\{2\ 0\ -1\}$ ,  $\{1\ 1\ -1\}$ ,  $\{1\ -1\ 0\}$  forms are observed, while  $\{1\ 1\ -2\}$  and  $\{2\ 0\ -1\}$  forms are absent in the experimental habit and all these forms have the lowest attachment energies, which represent F-faces of the crystal habit. These effects are independent of the force field parameters. Because of the extra extinction condition the forms  $\{1\ 1\ -2\}$  and  $\{2\ 0\ -1\}$  are not permitted and do not show up in the experimental habit. However, the attachment energies of  $\{1\ 1\ -2\}$  and  $\{2\ 0\ -1\}$  would cause this face to appear in the growth morphology.

For the vitamin C crystal habits, we found the same face forms for the Momany, Lifson, Scheraga and Dreiding force fields (see Figures 12-14). These forms are observed in experimentally grown crystals from water, isopropyl alcohol and isopropyl alcohol-methanol. For all 4 force fields the attachment energies for both the  $\{0\ 0\ 1\}$  and  $\{1\ 0\ 0\}$  are very close to the threshold value for appearance in the morphology. Therefore, they are very sensitive to changes in the force field parameters. In the case of the Momany and Scheraga and Dreiding force fields, the  $\{0\ 2\ 0\}$  does not show up for crystal growth from acetone-water, but the  $\{0\ 2\ 0\}$  form does show up for the Lifson force field (see Figure 15). The crystal shape, in the case of the Momany, Lifson and Scheraga force fields, was elongated along the B-axis compared to the crystal growth

form. This is in agreement with experimental crystal habits.

## Conclusions

The ability to understand the external shape of crystals has wide and varied applications in both the fundamental and applied aspects of crystal science. A basic approach to the presence of potential hydrogen bonding polar solvents has been presented. This work demonstrates the utility of combining molecular modeling and experimental data to solve molecular structures in the case of organic structures. It has been shown that hydrogen bonding can strongly affect the crystal habit of organic molecules. Both lattice geometry and attachment energy methods predict the vitamin C crystal habit that approximates growth morphologies. There are, however, significant differences between predicted and observed morphologies, which are likely caused by hydrogen bonding between solvent molecules and crystal faces. The changes in the morphologies of crystals caused by solvents of varying polarity are generally consistent with the interpretation that hydrogen bonding between solvents and crystal faces causes these changes and the departure from predicted morphologies. It is also concluded that, in general, the theoretical crystal habits based on dimer PBC analysis are in good agreement with the experimental morphology.

## Acknowledgment

This study was supported by Kafkas University, Kars, Turkey, and the Highly Filled Material Institute, Stevens Institute of Technology, USA.

## References

1. T. Nogrady, **Medicinal Chem. Biochem. Approach**. Second Ed., Oxford University Press, (1988).
2. H.R. Karfunkel, B. Rohde, F.J.J. Leusen, R.J. Gdanitz and G.J. Rihs, **Comput. Chem.**, **14**, 1125 (1993).
3. P. Bennema, **Growth and Morphology of Crystals: Integration of Theories of Roughening and Hartman-Perdok Theory**, Ed. D.T.J. Hurle, North Holland: Amsterdam, 1, 477 (1993).
4. P.A. Seib and B.M. Tolbert, **Ascorbic Acid: Chemistry, Metabolism, and Uses**. **Am. Chem. Soc.**, Washington, D.C. 1982.
5. J. Hvoslef, **Acta Chem. Scand.** **18**, 841 (1964).
6. J. Hvoslef, **Acta Crystallogr. Sect.**, **B24**, 23 (1968).
7. V. Sudhakar, T.N. Bhat and M. Vijayan, **Crystallogr. Sec.** **B36**, 125 (1980).
8. W.T.M. Mooij, B.P.V. Eijck, S. Price, L. Verwer, P. Verwer and J. Kroon, **J. Comput. Chem.**, **19**, 459 (1998).
9. R.F.P. Grimbergen and P.J. Bennema, **J. Am. Chem. Soc.**, **35**, 30 (1996).
10. P. Hartman and P. Bennema, **J. Cryst. Growth**, **49**, 145 (1980).
11. R. Ginde and A.S. Myserson, **J. Cryst. Growth**, **126**, 216 (1993).
12. J.D.H. Donnay, and D. Harker, **Am. Mineral.**, **22**, 463 (1937).
13. P. Hartman and W.G. Perdok, **Acta Cryst.**, **8**, 49 (1955).

14. S.L. Mayo, B.D. Olafson and W.A. Goddard, **J. Phys. Chem.**, **94**, 8897 (1990).
15. F.A. Momany, L.M. Carruther, R.F. McGuire and H.A. Scheraga, **J. Phys. Chem.**, **78**, 1579 (1974).
16. Molecular Simulation Incorporated, Inc., **Cerius<sup>2</sup> Molecular Modeling Package** Suite, San Diego, CA, 1998.
17. S. Lifson, A.T. Hagler and P. Dauber, **J. Am. Chem. Soc.**, **101**, 5111 (1979).
18. G. Nemethy, M.S. Pottle and H.A. Scheraga, **J. Phys. Chem.** **87**, 1883 (1983).
19. A. Bravais, **Etudes Crystallographiques**, Paris, France, (1913).